PHYSICAL REVIEW B VOLUME 24, NUMBER 12 15 DECEMBER 1981

Adsorption of molecular nitrogen on nickel. I. Cluster-model theoretical studies

K. Hermann,* P. S. Bagus, C. R. Brundle, and D. Menzel†
IBM Research Laboratory, San Jose, California 95193
(Received 6 February 1981)

Hartree-Fock calculations on a linear cluster, NiN_2, have been performed. Self-consistent-field calculations on the ground and hole states of the cluster and the free N_2 molecule have been used to determine the shifts in valence ionization potentials (IP) of N_2 when it is bound to a Ni atom. The understanding of these shifts is an important contribution to the analysis of the valence-level photoemission spectrum of N_2 adsorbed on Ni, even though additional effects are likely here because of the extended metal surface. We can explain, on the basis of the bonding characteristics, why the $2\sigma_u$-$3\sigma_g$ N_2 IP separation increases when N_2 is bonded to a Ni atom, whereas the equivalent IP separation in a NiCO cluster decreases compared with free CO. We demonstrate also that one of the extra effects of a real surface is that significant backbonding from Ni $4p\pi$ levels to the empty π^* N_2 orbital is possible. Such a bonding contribution in a NiN_2 cluster can only be included by choosing a separated Ni atom configuration containing $4p\pi$ character. When this is done, the self-consistent calculations of the Ni atom in this configuration bonded to an N_2 molecule reveal significant $4p\pi$-π^* backbonding in addition to the approximately equal σ-bonding contributions from the $2\sigma_u$ and $3\sigma_g$ orbitals of N_2. The inclusion of the π^* backbonding reduces the N_2-derived valence IP's by some 2.5 eV. The theoretical results for NiN_2 are compared with those for NiCO in order to facilitate the comparison of the photoemission results for the Ni(100)/N_2 and Ni(100)/CO systems, which is discussed in detail in the following paper.

I. INTRODUCTION

CO adsorption on Ni has been extensively studied by uv photoemission experiments. It has been the prototype system for interpretation of the adsorbate resonance orbital structure observed for adsorption of CO on metals. The original correlations between the adsorbate-induced features and the molecular orbitals of free CO proved subsequently to be in error.[1,2] The correct assignment was arrived at by a combination of cluster calculations of orbital energies,[3] sensible comparison to photoemission data of organometallics,[4] the realization that changes in photoemission final-state relaxation energies for the adsorbed situation could be as important as ground-state electronic effects,[5] and photon and angular-dependent studies which established the π and σ character of the observed CO-induced features.[6] More recently, detailed *ab initio* Hartree-Fock (HF) calculations on the ground and the CO-like hole states of the simple model cluster NiCO (Refs. 1 and 7) have yielded more insight into the nature of the bonding and of the relative contributions of initial and final-state effects to the observed ionization potentials (IP) of valence or core hole states. It is interesting both experimentally and theoretically to study the changes occurring by substituting the isoelectronic molecule N_2 for CO. Nitrogen chemisorbs molecularly on Ni and W at low temperatures, the heat of adsorption being considerably lower than for CO. X-ray- and ultraviolet-photoemission-spectroscopy (XPS and UPS) investigations[8] of N_2 adsorbed on W(110) and on Ni(100) suggest that the N_2 is adsorbed vertically. We therefore investigate the linear Ni-N-N cluster as a model for these adsorption systems. As in linear NiCO, the electronic structure of NiN_2 is determined by *ab initio* Hartree-Fock calculations. The main questions we address in this paper are the following:

(1) What is the bonding mechanism in the cluster Ni-N_2; i.e., which orbitals are primarily involved in the bonding?

(2) What are the differences in the ground-state electronic structure compared to the cluster NiCO?

(3) What are the photoemission final-state effects and how do they compare to NiCO?

(4) How do the combined initial- and final-state

effects affect the N_2 and CO-derived valence-level IP's when bonded to a Ni atom in a linear cluster.

We show in the following paper[9] that the differences between NiNN and NiCO linear clusters can, in areas (1)—(4) above, explain the main experimental trends in a comparison of the valence-level photoemission spectra of CO; CO/Ni(100); N_2 and N_2/Ni(100). This again demonstrates the applicability of the linear cluster-model calculations to the interpretation of uv photoemission data of real adsorption situations.

The N 1*s* core-level spectra[8] for N_2 on Ni(100) and W(110) show very strong satellite structure which has been explained theoretically by screening effects arising when the core hole is created.[10] We have found that these core-hole screening effects can also be theoretically described using a linear NiN_2 cluster and *ab initio* Hartree-Fock self-consistent-field (HF ΔSCF) calculations in which there are no adjustable parameters other than choosing appropriate electronic configurations and, of course, performing the calculation as a function of Ni—N_2 bond distance.[11,12] In the present paper we deal with the valence ionizations, but we point out that our conclusions here concerning the role of Ni $4p\pi$-$N_2\pi^*$ backbonding are also borne out by the core-level results which cannot be explained without such a bonding contribution.[8—12] In Sec. II we give the computational details and in Sec. III we present our results from the model calculations. Section III A describes the ground-state electronic properties while Sec. III B discusses the valence-level ionization potentials of N_2 and the N_2-derived levels in NiN_2. In Sec. IV we summarize the conclusions of our cluster-model studies stressing those features which are pertinent for comparison with adsorption experiments, which is done in the following paper.[9]

II. COMPUTATIONAL DETAILS

Nickel dinitrogen compound molecules, which could give an indication of the appropriate interatomic distances to use in the linear cluster, do not seem to exist. Thus for the Ni—N distance, d_{Ni-N}, in NiN_2 the sum of atomic radii[13] was taken ($d_{Ni-N}=3.80$ bohrs) for the first calculation, while for d_{N-N} the value of the free molecule[14] (2.074 bohrs) was used. In order to study the dependence of the cluster properties on its geometry, calculations have been performed with various distances d_{Ni-N}. The effect on the electronic structure due to reasonable variations, $\sim 5\%$, of d_{Ni-N} about the sum of the covalent radii is rather small, as will be seen later.

SCF analytic basis-set Hartree-Fock calculations for various electronic states of the cluster and for the free N_2 molecule were carried out following the Roothaan approach as implemented in the program system MOLALCH.[15] The contracted Gaussian basis set for N was taken from van Duijneveldt's calculations[16] on the free atom. Here 9*s* and 5*p* functions were contracted to (4,3), and a *d* function (exponent $\alpha=1.0$) (Ref. 17) has been added. The basis set for Ni was taken from Wachter's calculations[18] on the atom, to which two *p* functions (exponents $\alpha=0.228$ and $\alpha=0.08$) were added to allow for *p* hybridization of the Ni 4*s* orbital. This basis set is identical to the one used for Ni in a previous cluster study on NiCO.[1] On the whole, the basis sets used in the present calculation are of better than "double-zeta" quality,[19] and it is very unlikely that the results will change significantly if larger basis sets are used.

III. THEORETICAL RESULTS

A. Ground-state electronic properties

In our analysis we are particularly concerned with comparing the properties of the nickel—nitrogen bonding with those of the nickel—carbon monoxide bonding. For this reason, we shall review in this section some aspects of previous results[1] for the NiCO cluster as well as presenting our NiN_2 cluster results. Our bonding analysis is also based on comparisons between properties of the free molecule and of the molecule in the cluster, and we will thus also present results for free CO and N_2.

In Tables IA and IB, we report some properties of CO and N_2, respectively. For each molecule we give the total energy and the orbital energies, gross and overlap populations obtained with a Mulliken population analysis,[20] and expectation values of *z*, the distance along the internuclear axis. For CO, the bond distance is 2.173 bohrs, which is the experimental distance for CO in $Ni(CO)_4$ and was also used for the NiCO cluster. This is only slightly larger than the experimental free CO bond distance of 2.132 bohrs. The ground-state electronic configuration of CO is $1\sigma^2 2\sigma^2 3\sigma^2 4\sigma^2 1\pi^4 5\sigma^2$. The 1σ and 2σ orbitals are the O 1*s* and C 1*s* core levels, respectively. The 3σ orbital is composed primarily of O 2*s* and some C 2*s* character. The

TABLE IA. Properties of the CO-molecule wave function including orbital energies ϵ, gross and overlap populations, and expectation values of the distance along the internuclear axis $\langle z \rangle$. For each orbital, the gross and overlap populations are normalized to one electron and gross populations are decomposed in s, p, and d character. The $\langle z \rangle$ are given both with respect to the carbon atom as origin, $\langle z \rangle_C$, and with respect to oxygen as origin, $\langle z \rangle_O$. The carbon atom is placed 2.173 bohrs to the left of oxygen. All values are in atomic units. The total energy is $E_{tot} = -112.764\,694$.

Orbital	ϵ	$\langle z \rangle_C$	$\langle z \rangle_O$		Gross population C	Gross population O	Overlap population C–O
1σ(O 1s)	−20.669	2.173	0.000	s	0.00	1.00	
				total	0.00	1.00	0.00
2σ(C 1s)	−11.370	0.000	−2.173	s	1.00	0.00	
				total	1.00	0.00	0.00
3σ	−1.510	1.589	−0.584	s	0.14	0.70	
				p	0.09	0.07	
				d	0.01	0.00	
				total	0.23	0.77	0.28
4σ	−0.801	2.128	−0.045	s	0.19	0.21	
				p	0.02	0.58	
				d	0.00	0.00	
				total	0.21	0.79	0.06
5σ	−0.557	−0.441	−2.614	s	0.57	−0.01	
				p	0.35	0.09	
				d	0.00	0.00	
				total	0.92	0.08	−0.18
1π	−0.629	1.665	−0.508	p	0.22	0.76	
				d	0.01	0.01	
				total	0.23	0.77	0.20
Total population				s	3.79	3.80	
				p	1.82	4.51	
				d	0.05	0.04	
				total	5.65	8.35	

center of charge lies closer to oxygen than to carbon, and the overlap population indicates substantial bonding character. The 4σ and 5σ orbitals are "lone pairs" on oxygen and carbon, respectively, as may be seen from the values of $\langle z \rangle$. The 1π is dominantly composed of O $2p$ and contributes, with the 3σ orbital, to the CO triple bond. This description of the character of the molecular orbitals (MO's) is schematically represented in Fig. 1.

The MO's of the ground state of N_2 belong to representations of $D_{\infty h}$ and are either symmetric (g) or antisymmetric (u) with respect to inversion through the center of the molecule. In Table IB, we have denoted the N_2 MO's with both $D_{\infty h}$ and $C_{\infty v}$ designations. We shall, in the following, use the $C_{\infty v}$ rather than the $D_{\infty h}$ MO designations in order to facilitate comparison with CO and also with the NiN_2 cluster, where the two nitrogen atoms are inequivalent. For N_2, the populations of the two nitrogen atoms are identical and the center of charge for each MO, $\langle z \rangle$, is at the inversion center. The results in Table IB are for the experimental internuclear distance, $r(N-N) = 2.074$ bohrs. As was the case for CO, the N_2 triple bond is formed by the $3\sigma(2\sigma_g)$ and $1\pi(1\pi_u)$ MO's. The overlap populations indicate that the $4\sigma(2\sigma_u)$ MO is antibonding, and that the $5\sigma(3\sigma_g)$ MO is essentially nonbonding. The small negative value of the 5σ overlap population arises from the relative signs (and magnitudes) of the N s and N p contributions as shown in Fig. 1. In fact, it is quite reasonable to regard the 4σ and 5σ MO's as even and odd

TABLE IB. Properties of the N_2-molecule wave function. The nitrogen denoted N_a is 2.074 bohrs to the left of the second nitrogen, N_b, and $E_{tot} = -108.966\,141$. See the heading of Table IA for further details.

Orbital				Gross population		Overlap population
$C_{\infty v}$	$D_{\infty h}$	ϵ	$\langle z \rangle_{N_a}$		N_a	$N_a - N_b$
1σ	$1\sigma_g$	−15.678	1.037	s	0.50	
				total	0.50	0.00
2σ	$1\sigma_u$	−15.675	1.037	s	0.50	
				total	0.50	0.00
3σ	$2\sigma_g$	−1.472	1.037	s	0.38	
				p	0.12	
				d	0.01	
				total	0.50	0.40
4σ	$2\sigma_u$	−0.775	1.037	s	0.36	
				p	0.14	
				d	0.00	
				total	0.50	−0.20
5σ	$3\sigma_g$	−0.630	1.037	s	0.15	
				p	0.34	
				d	0.01	
				total	0.50	−0.03
1π	$1\pi_u$	−0.611	1.037	p	0.49	
				d	0.01	
				total	0.50	0.26
Total population				s	3.77	
				p	3.17	
				d	0.06	
				total	7.00	

combinations, respectively, of lone pairs on the nitrogen atoms, as may be seen in Fig. 1. This description is also supported by considering the $\langle z^2 \rangle$ taken with respect to the inversion center. The values of $\langle z^2 \rangle_{4\sigma} = 3.28$ and $\langle z \rangle_{5\sigma} = 3.43$ bohr^2 are much larger than the square of the distance to a nitrogen atom, $(1.037)^2 = 1.08$. This indicates that a substantial amount of charge lies outside of the N atoms, as would be expected for lone-pair orbitals. For comparison, $\langle z^2 \rangle = 0.57$ bohr^2 for the bonding 3σ MO.

Figure 1 also shows that it is physically reasonable to make the correspondence between the orbitals of CO and N_2 which was implied by our choice of $C_{\infty v}$ designations for the valence MO's of N_2. The corresponding CO and N_2 MO's have the same "symmetry" in the sense that the relative signs of the atomic-orbital contributions to the MO's are the same even though their magnitudes are different.

Hartree-Fock calculations were performed for various electronic configurations of the NiN_2 cluster for $d_{Ni-N} = 3.80$ bohrs in order to determine the ground state of the cluster. The ground-state configuration obtained was used for calculations at all other Ni−N distances and as the reference configuration for removing electrons to form ionic states. It was determined to be a $^3\Delta$ state with the configuration

$$\text{core}\ 8\sigma^2(\tilde{3}\sigma)9\sigma^2(\tilde{4}\sigma)10\sigma^2(\tilde{5}\sigma)11\sigma^2(3d\sigma)$$
$$12\sigma^1(4sp\sigma)3\pi^4(\tilde{1}\pi)4\pi^4(3d\pi)1\delta^3(3d\delta)\,, \qquad (1)$$

where the core includes the $1s^2$ to $3p^6$ orbitals of Ni and the $1s^2$ orbitals of N. The designations in parentheses denote the principal character (in terms of Ni and N_2 contributions) of each of the orbitals. In the linear cluster, the N_2-like orbitals retain

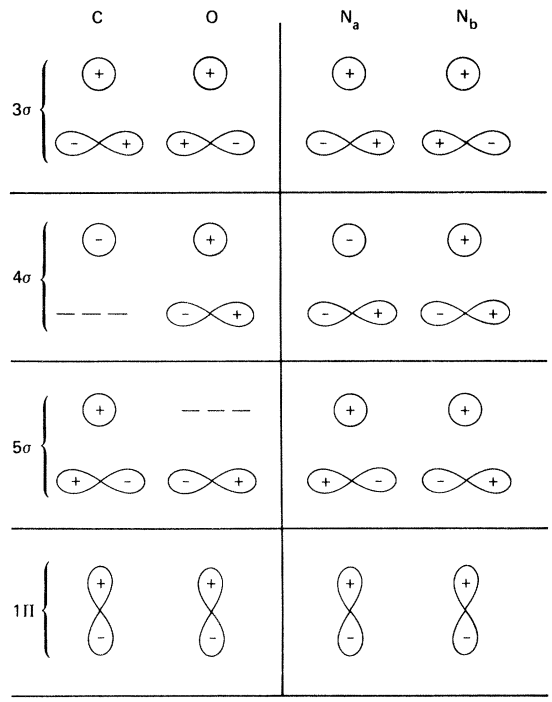

FIG. 1. Schematic representation of the relative phases of the atomic orbital s and p characters of the CO and N_2 valence MO's. The s character is denoted by a circle and the sign is that for the outer, $2s$, region. When the magnitude of the character is very small (Mulliken net population less than 0.01), it is omitted from the figure. Otherwise, no attempt is made to show the magnitudes of the various contributions.

much of their molecular character and are denoted with an added tilde: $\tilde{3}\sigma$, $\tilde{4}\sigma$, etc. The 11σ, 4π, and 1δ MO's are predominantly Ni $3d$-like. The singly occupied 12σ is a Ni $4s$-$4p$ hybrid directed to form a lone pair. The same ground state was found for the isoelectronic NiCO cluster.[1,7] However, there are significant differences in the characters of the MO's between NiCO and NiN_2. In Tables IIA and IIB we report some properties of the NiCO and NiN_2 wave functions, respectively. The results in Table II are for $r(\text{Ni}-\text{C})=3.477$ bohrs, the bond distance in $Ni(CO)_4$, and $r(\text{Ni}-\text{N}_a)=3.80$ bohrs. (We denote the nitrogen atom nearest to the Ni by N_a and the one furthest away by N_b.) The orbital properties are given only for the free molecule derived $\tilde{1}\sigma$ to $\tilde{5}\sigma$ and $\tilde{1}\pi$, and for the Ni $3d$ and $4sp$-like orbitals.

The properties given in Table II support, for both NiCO and NiN_2 clusters, the general characterization of the valence MO's given above. The $\tilde{3}\sigma$ and $\tilde{1}\pi$ MO's are only very slightly affected by the presence of the Ni atom in that the major change seems to be reflected in the center of charge (see $\langle z\rangle_C$ or $\langle z\rangle_{N_a}$), which moves slightly toward Ni (by ~ 0.01 bohrs for $\tilde{3}\sigma$ and by 0.1 bohrs for $\tilde{1}\pi$). The overlap populations, Ni—C or Ni—N_a are zero for both MO's, indicating that they are essentially nonbonding to the nickel.

For $\tilde{4}\sigma$ and $\tilde{5}\sigma$, the effect of the Ni atom is somewhat larger and is also different for the two clusters. For NiCO, the $\tilde{4}\sigma$ (being largely an O lone pair in free CO) is a slightly antibonding orbital with respect to Ni. The $\tilde{5}\sigma$ (being largely a C lone pair in free CO) has acquired 13% Ni character (11% $3d\sigma$) and has the largest Ni—C overlap population. This would indicate that the $\tilde{5}\sigma$ is primarily responsible for the bonding of CO to the Ni atom in the ground state of the NiCO linear cluster. For NiN_2, both the $\tilde{4}\sigma$ and $\tilde{5}\sigma$ are involved in the bonding to Ni and, judging from the Ni—N_a overlap population, are bonding to about the same extent. This also can be related to the free-molecule character of 4σ and 5σ in N_2. Here both MO's have lone-pair character on N_a (see Fig. 1) and hence may easily interact with Ni. The $\tilde{4}\sigma$ and $\tilde{5}\sigma$ become asymmetric with the center of charge of $\tilde{4}\sigma$ shifted toward the Ni atom and that of $\tilde{5}\sigma$ shifted away; for both MO's the shift is ~ 0.5 bohrs.

For both clusters there is some small amount of $d\pi$ to $2\pi^*$ backbonding in the $3d\pi$ MO, leading to a contribution of this orbital to the bonding. The total amount of $2\pi^*$ character in the cluster is defined as the excess of the π population of the molecule over the value of 4 which is assumed to correspond to $1\pi^4 2\pi^0$. For NiCO the $2\pi^*$ occupation is 0.18 electrons; for NiN_2 it is only 0.07. This indicates that there is a larger $d\pi$ to $2\pi^*$ bonding contribution in NiCO. For NiN_2, both the $3d\sigma$ and $4sp\sigma$ are more antibonding than is the case for NiCO. This also should contribute to a weaker total interaction between Ni and N_2 than between Ni and CO. In both clusters, the $3d\delta$ makes no contribution to the bond. The total gross population analysis gives an almost neutral Ni atom and only slightly modified total populations on the "ad-molecule".

The results discussed above suggest that the bonding of the ad-molecule, N_2 or CO, with the Ni atom is rather weak. We define, as usual, the SCF binding energy, ΔE_{SCF}, as the difference between the sum of the SCF energies of the Ni atom and the free molecule and the SCF energy of the clus-

TABLE IIA. Properties of the NiCO cluster ground-state wave function. Orbital properties are given only for the free molecule derived and the Ni $3d$ and $4sp$-like orbitals. The linear cluster lies along the z axis with the Ni atom on the left end and the O atom on the right. The quantities tabulated are defined in the heading of Table IA.
$E_{tot}=-1619.346\,137$, $r(\text{Ni}-\text{C})=3.477$, and $r(\text{C}-\text{O})=2.173$.

Orbital	ϵ	$\langle z\rangle_{Ni}$	$\langle z\rangle_C$		Gross population Ni	C	O	Overlap population Ni—C	C—O
$\tilde{1}\sigma$(O 1s)	−20.709	5.650	2.173	s	0.00	0.00	1.00		
				total	0.00	0.00	1.00	0.00	0.00
$\tilde{2}\sigma$(O 1s)	−11.422	3.478	0.001	s	0.00	1.00	0.00		
				total	0.00	1.00	0.00	0.00	0.00
$\tilde{3}\sigma$	−1.547	5.056	1.579	s	0.00	0.14	0.69		
				p	0.00	0.09	0.07		
				d	0.00	0.01	0.00		
				total	0.00	0.24	0.76	0.00	0.29
$\tilde{4}\sigma$	−0.846	5.260	1.783	s	−0.01	0.27	0.20		
				p	0.00	0.04	0.49		
				d	0.01	0.00	0.00		
				total	0.00	0.31	0.69	−0.02	0.06
$\tilde{5}\sigma$	−0.685	3.054	−0.423	s	0.01	0.35	0.01		
				p	0.01	0.35	0.16		
				d	0.11	0.00	0.00		
				total	0.13	0.71	0.17	0.07	−0.06
$3d\sigma$	−0.410	0.266		s	0.16	0.01	0.00		
				p	0.04	0.00	0.01		
				d	0.79	0.00	0.00		
				total	0.98	0.01	0.01	0.00	0.00
$4sp$	−0.209	−1.586		s	0.66	0.01	0.00		
				p	0.26	0.02	0.00		
				d	0.04	0.00	0.00		
				total	0.97	0.03	0.00	−0.03	−0.04
$\tilde{1}\pi$	−0.672	5.005	1.528	p	0.00	0.26	0.72		
				d	0.01	0.01	0.01		
				total	0.01	0.26	0.72	0.00	0.21
$3d\pi$	−0.462	0.269		p	0.00	0.02	0.04		
				d	0.94	0.00	0.00		
				total	0.94	0.02	0.04	0.02	−0.03
$3d\delta$[a]	−0.543	0.000		d	1.00	0.00	0.00		
				total	1.00	0.00	0.00	0.00	0.00
Total population				s	6.98	3.56	3.80		
				p	12.36	2.09	4.44		
				d	8.67	0.06	0.04		
				total	28.01	5.71	8.28		

[a]Equivalence restriction (Ref. 35) maintained for the xy and x^2-y^2 components of the δ-molecular orbital.

ter; e.g.,

$$\Delta E_{SCF}(NiN_2)=E_{SCF}(Ni)+E_{SCF}(N_2)-E_{SCF}(NiN_2)\,. \quad (2)$$

For the Ni atom, the SCF energy of the $3d^9 4s^1(^3D)$ state is the appropriate choice since this state is most like that found for Ni in the cluster. We find that $\Delta E_{SCF}(NiCO)=0.03$ eV for

TABLE IIB. Properties of the NiN_2 cluster ground-state (GS) wave function. The cluster lies along the z axis with the Ni atom on the left; N_a denotes the central nitrogen and N_b the nitrogen on the right. See the heading of Table IA for definitions of the quantities tabulated. $E_{tot}=-1615.547\,168$, $r(Ni-N_a)=3.80$, and $r(N_a-N_b)=2.074$.

Orbital	ϵ	$\langle z\rangle_{Ni}$	$\langle z\rangle_{N_a}$		Gross population Ni	Gross population N_a	Gross population N_b	Overlap population $Ni-N_a$	Overlap population N_a-N_b
$\tilde{1}\sigma$(N 1s)	−15.731	4.848	1.048	s	0.00	0.49	0.51		
				total	0.00	0.49	0.51	0.00	0.00
$\tilde{2}\sigma$(N 1s)	−15.728	4.826	1.026	s	0.00	0.51	0.49		
				total	0.00	0.51	0.49	0.00	0.00
$\tilde{3}\sigma$	−1.521	4.822	1.022	s	0.00	0.38	0.40		
				p	0.00	0.10	0.12		
				d	0.00	0.01	0.01		
				total	0.00	0.48	0.52	−0.01	0.39
$\tilde{4}\sigma$	−0.848	4.205	0.405	s	0.01	0.40	0.28		
				p	0.01	0.23	0.06		
				d	0.02	0.00	0.00		
				total	0.03	0.63	0.34	0.03	−0.19
$\tilde{5}\sigma$	−0.697	5.348	1.548	s	0.01	0.07	0.23		
				p	0.01	0.25	0.41		
				d	0.02	0.00	0.00		
				total	0.03	0.32	0.65	0.03	−0.03
$3d\sigma$	−0.370	0.108		s	0.14	0.01	−0.01		
				p	0.02	−0.02	0.00		
				d	0.86	0.00	0.00		
				total	1.01	−0.01	−0.01	−0.02	−0.09
$4sp$	−0.206	−1.306		s	0.76	0.00	0.00		
				p	0.15	0.02	0.00		
				d	0.06	0.00	0.00		
				total	0.98	0.02	0.00	−0.07	−0.06
$\tilde{1}\pi$	−0.663	4.730	0.930	p	0.00	0.52	0.45		
				d	0.01	0.01	0.01		
				total	0.01	0.53	0.46	0.00	0.26
$3d\pi$	−0.423	0.132		p	0.00	0.00	0.02		
				d	0.97	0.00	0.00		
				total	0.97	0.01	0.02	0.01	−0.01
$3d\delta$[a] (x^2-y^2)	−0.471	0.00		d	1.00	0.00	0.00		
$3d\delta$[a] (xy)	−0.533			total	1.00	0.00	0.00	0.00	0.00
Total population				s	7.06	3.71	3.80		
				p	12.22	3.25	3.08		
				d	8.77	0.05	0.06		
				total	28.05	7.01	6.94		

[a]The equivalence restriction (Ref. 35) for the x^2-y^2 and xy components was not maintained. The $d\delta(x^2-y^2)$ was doubly occupied and the $d\delta(xy)$ was singly occupied.

$r(Ni-C)=3.477$ bohrs and $\Delta E_{SCF}(NiN_2)=0.01$ eV for $r(Ni-N_a)=3.80$ bohrs. If the Ni-to-molecule distance is increased, the binding energy increases somewhat. At the SCF equilibrium separation of Ni and C, 3.92 bohrs, $\Delta E_{SCF}(NiCO)=0.20$ eV,[1] and at the largest distance for which we performed NiN_2 calculations, $r(Ni-N_a)=4.20$ bohrs, $\Delta E_{SCF}=0.09$ eV. These

values are clearly much smaller than the heats of adsorption of CO on Ni, ~ 1.3 eV,[21] and N_2 on Ni, ~ 0.5 eV,[22] and also have a minimum in the total energy at larger bond distances.

The symmetry of the linear clusters does not permit any interaction of the Ni $4sp$ valence level with the adsorbate $2\pi^*$ orbital in the cluster ground state because this Ni level has σ symmetry [see Eq. (1)]. Such an interaction may have importance, however, for a Ni surface and could contribute to the bond strength. Schönhammer and Gunnarson[10(a)] have shown theoretically, using a model Hamiltonian for an adsorbate molecule on a metal, that the extent of coupling between metal valence levels and an empty adsorbate valence level lying near E_F has a dramatic effect on the line shape of the adsorbate core-level photoemission. The mechanism involves electron transfer from the metal into the adsorbate valence level in the final core-hole photoemission state in an attempt by the system to screen the localized adsorbate core hole. It was subsequently shown by Fuggle *et al.*[8(b)] that the mechanism explains the apparently very anomalous adsorbate core line shapes for CO adsorbed on Cu and N_2 adsorbed on Ni and W. The adsorbate screening orbital in these cases is the $2\pi^*$ level. Further calculations by Schönhammer and Gunnarson[10(b)] using a parametrized Anderson Hamiltonian showed that for the specific case of CO on Cu(100) obtaining good agreement between theoretical and experimental line shapes required that the dominant contribution from the metal to $2\pi^*$ coupling come from the metal *sp* levels, *not d*, levels.

It is clearly evident from the work reported above that the Ni $4sp-N_2 2\pi^*$ coupling is important for N_2 chemisorbed on Ni. It therefore becomes necessary in trying to make a connection between the chemical bonding and theoretical photoemission spectra of the linear cluster on the one hand, and the experimental results for N_2/Ni(100) (Ref. 9) on the other, that some scheme be devised for allowing a Ni $4sp$-$N_2 2\pi^*$ interaction in the linear cluster. This can be achieved by constructing an artificial ground state of the cluster from an excited configuration of the separated Ni atom in which the $4p\pi$ orbital is occupied (this state of the Ni atom is ~ 1.5 eV above the ground state). The cluster is then in a triplet state[23] with the configuration

$$\text{core}\ 8\sigma^2(\tilde{3}\sigma)9\sigma^2(\tilde{4}\sigma)10\sigma^2(\tilde{5}\sigma)11\sigma^2(3d\sigma)$$
$$3\pi^4(\tilde{1}\pi)4\pi^4(3d\pi)5\pi^1(4p\pi)1\delta^3(3d\delta)\ . \qquad (3)$$

From now on we shall denote this artificial "ground state" as GS(π) and the true ground state of the linear cluster as GS. Results on GS(π) have been presented for both NiCO (Ref. 11) and NiN_2 (Ref. 12), with the object of interpreting the nature of the photoionization peaks of the molecular core levels. GS(π), since it contains only π character for the Ni valence electron, should exaggerate the importance of the Ni metal *sp* valence to $2\pi^*$ bonding. Our work on the core levels has shown,[11,12] by comparison with experiment,[9] that this is indeed so and that this overestimate may be partially compensated by considering an increased Ni to molecule bond distance. In Table III, we present results for the GS(π) of NiN_2 for $r(\text{Ni}-\text{N}_a)=4.20$ bohrs. This distance was chosen because it gives reasonable relative intensities for the fully relaxed and satellite N $1s$ core-level peaks compared to the experimental results for N_2 on Ni(100).[12] However, the differences between GS and GS(π) to be discussed below do not depend strongly on the $\text{Ni}-\text{N}_a$ distance.

It is clear from Table III that the $4p\pi$ cluster molecular orbital, 5π in Eq. (3), does contain a large $N_2 2\pi^*$ admixture and that this orbital contributes significantly to the bond between Ni and N_2 in GS(π). As a consequence, we find that the cluster is bound by 1.13 eV with respect to the separated Ni atom ($3d^9 4p$) and N_2 molecule. This is now larger than the heat of adsorption of N_2 on Ni, as expected, since the GS(π) overestimates the amount of π character to be found in the real Ni-metal *sp* valence band.[24]

Two features of the GS(π) wave function are of particular importance for the analysis of the IP's of the N_2-derived levels to be presented later. (1) The characters of the N_2 valence levels, $\tilde{3}\sigma$, $\tilde{4}\sigma$, $\tilde{5}\sigma$, and $\tilde{1}\pi$ are very similar to those of GS. This may be seen by comparing the $\langle z \rangle$ and the gross and overlap populations between Tables IIB and III. The small differences obtained are, in fact, partly accounted for by the difference in $\text{Ni}-\text{N}_a$ distance between the two states. (2) The orbital energies ϵ of *all* of the N_2-derived levels are shifted almost uniformly by ~ 2.4 eV to lower (nearer to zero) values. The shift is remarkably constant for the valence σ levels and is only 0.25 eV smaller for the $\tilde{1}\pi$ level. It arises because the occupation of $2\pi^*$ by ~ 0.3 electrons, leads to a slightly negative N_2 (see Table III), thus raising the energies of these levels.

We note also that the $3d\pi$ and $3d\sigma$ levels are slightly changed in GS(π). The backbonding of

TABLE III. Properties of the NiN_2 cluster wave function for the artificial ground state denoted GS(π) [see Eq. (3)]. $E_{tot} = -1615.459\,820$, $r(Ni-N_a) = 4.20$, and $r(N_a-N_b) = 2.074$.

Orbital	ϵ	$\langle z\rangle_{Ni}$	$\langle z\rangle_{N_a}$		Gross population Ni	N_a	N_b	Overlap population Ni–N_a	Na–N_b
$\tilde{1}\sigma$(N 1s)	−15.645	4.216	0.016	s	0.00	0.99	0.01		
				total	0.00	0.99	0.01	0.00	0.00
$\tilde{2}\sigma$(N 1s)	−15.625	6.258	2.058	s	0.00	0.01	0.99		
				total	0.00	0.01	0.99	0.00	0.00
$\tilde{3}\sigma$	−1.431	5.220	1.020	s	0.00	0.38	0.39		
				p	0.00	0.10	0.12		
				d	0.00	0.01	0.01		
				total	0.00	0.49	0.52	0.00	0.39
$\tilde{4}\sigma$	−0.758	4.670	0.470	s	0.01	0.38	0.28		
				p	0.01	0.23	0.08		
				d	0.01	0.00	0.00		
				total	0.03	0.62	0.36	0.04	−0.14
$\tilde{5}\sigma$	−0.606	5.638	1.438	s	0.01	0.07	0.23		
				p	0.01	0.26	0.40		
				d	0.02	0.00	0.00		
				total	0.04	0.33	0.63	0.04	−0.04
$3d\sigma$	−0.406	0.100		s	0.05	0.01	−0.01		
				p	0.02	0.00	0.00		
				d	0.92	0.00	0.00		
				total	0.99	0.01	−0.01	0.01	−0.10
$\tilde{1}\pi$	−0.581	5.121	0.921	p	0.00	0.52	0.45		
				d	0.01	0.01	0.01		
				total	0.01	0.53	0.46	0.00	0.26
$3d\pi$	−0.445	0.069		p	0.00	0.00	0.01		
				d	0.98	0.00	0.00		
				total	0.99	0.00	0.01	0.00	0.00
$4p\pi$	−0.107	1.763	−2.437	p	0.68	0.14	0.17		
				d	0.00	0.00	0.00		
				total	0.68	0.14	0.17	0.16	−0.23
$3d\delta$[a] (x^2-y^2)	−0.489	0.000		d	1.00	0.00	0.00		
(xy)	−0.548			total	1.00	0.00	0.00	0.00	0.00
Total population				s	6.14	3.69	3.78		
				p	12.76	3.42	3.22		
				d	8.88	0.05	0.05		
				total	27.77	7.17	7.06		

[a]See footnote a to Table IIB.

$3d\pi$ to $2\pi^*$ is now essentially absent. This is reasonable since the $2\pi^*$ character on N_2 is now used for bonding to $4p\pi$. The $3d\sigma$ in GS(π) has a slightly bonding rather than antibonding character. The Ni 3d-like-level orbital energies shift to more negative values by ~0.5 to 1.0 eV owing to the small positive charge on Ni.

B. Valence-level ionization potentials of N_2 and NiN_2

The differences between the valence IP's of an adsorbate and those of the free molecule are often used as a means of delineating the electronic changes occurring on adsorption.[25,26] In a similar

spirit, we have calculated the ionization potentials for the N_2-like orbitals of the NiN_2 linear cluster and of free N_2 and compare them here. The ionization potentials are determined in two different approximations. First we determined the IP's in the frozen-orbital approximation where the orbitals are not allowed to relax in response to the removal of the ionized electron. For closed-shell systems, these values are just the negative HF eigenvalues. These values, referred to as I(Koopmans's), are given in Table IV for N_2. For open-shell systems such as NiN_2, coupling between the original unpaired electrons and the new unpaired electron left after ionization generates multiplet final states, and the frozen-orbital ionization potential to any one of these multiplet final states is now not exactly equal to $-\epsilon$.[27] The energy differences among the final multiplets arise from the exchange interactions among the open-shell electrons. For the clusters considered here, the largest exchange integrals are those between a valence N_2-like open-shell orbital and the 4sp-like Ni orbital, $12\sigma^1(4sp\sigma)$ for GS and $5\pi^1(4p\pi)$ for GS(π). A detailed discussion of the multiplet splitting is given in Ref. 1; here we wish to emphasize two essential points. First, the splitting is clearly primarily a cluster property which will not occur to any significant extent on a real metal surface since the metal 4sp conduction band does not contain unpaired spins. Second, even the cluster splitting is rather small as measured, say, by the difference between the high spin, quartet, state, and the center of gravity of the multiplet[1] denoted $\Delta\bar{E}_{MS}$. In the frozen-orbital approximation, the largest $\Delta\bar{E}_{MS}$ for the NiN_2 GS initial state is 0.1 eV for $\tilde{4}\sigma$ ionization. For the NiN_2 GS(π) initial state, the multiplet splittings are somewhat larger since the open Ni valence shell, $5\pi^1(4p\pi)$, has a fair amount of $N_2 2\pi^*$ character (see Table III), leading to larger exchange integrals.

TABLE IV. Computed and experimental ionization potentials, in eV, of the free N_2 molecule. The calculated values are for the experimental equilibrium internuclear distance, $r(N-N)=2.074$ bohrs.

Orbital	I(Koopmans's)	I(relaxed)	I(expt.)[a]
1σ(N 1s)	426.63	410.30[b]	409.9
2σ(N 1s)	426.53	410.30[b]	
3σ	40.07	37.73	37.3
4σ	21.09	20.18	18.6
5σ	17.15	15.89	15.5
1π	16.63	15.32	16.8

[a]K. Siegbahn *et al., ESCA Applied to Free Molecules* (North-Holland, Amsterdam, 1971).
[b]Calculations for the 1s holes were performed in $C_{\infty v}$, not $D_{\infty h}$ symmetry and the hole was found to be localized on one N atom.

However, even for GS(π), the largest values of $\Delta\bar{E}_{MS}$ for $\tilde{4}\sigma$ or $\tilde{1}\pi$ ionization, are still only 0.3 eV. For both these reasons, we consider only the high-spin final states for the calculation of the IP's. (For $\tilde{1}\pi$ ionization, we consider removal of a π_x electron which leads to a state which is a mixture of different $C_{\infty v}$ spatial symmetries.[1,23]) The cluster-frozen-orbital IP's, denoted I(Koopmans's), although differing slightly from $-\epsilon$, are given in Table V. For NiN_2 GS we report values for $d_{Ni-N_a}=3.65$, 3.80, and 4.00 bohr and for NiN_2 GS(π) for $d_{Ni-N_a}=4.20$ bohr.

In the second approximation, we have computed the SCF wave functions, for each final hole-state (high-spin quartet state) and taken the difference between the initial and final-state total energies. This procedure gives the relaxed IP, I(relaxed). The difference between I(Koopmans's) and I(relaxed) is equal to the final-state relaxation energy E_R. I(relaxed) values are given in Table IV for

TABLE V. Computed ionization potentials, in eV, of the N_2-like orbitals of linear NiN_2 for three different nickel-nitrogen distances. The notation I(Koopmans's) refers to the frozen orbital IP to a high-spin final state; I(relaxed) is obtained from differences of the Hartree-Fock total energies of the initial and self-consistent final high-spin states.

Orbital	I(Koopmans's)/GS			I(Koopmans's)/GS(π)	I(relaxed)/GS		
	r[a]=3.65	3.80	4.00	4.20	3.65	3.80	4.00
$\tilde{1}\sigma$(N 1s)	428.14	428.07	427.95	425.70	410.93	410.87	410.78
$\tilde{2}\sigma$(N 1s)	428.05	427.97	427.84	425.13	410.59	410.63	410.65
$\tilde{3}\sigma$	41.45	41.37	41.26	38.82	38.36	38.33	38.26
$\tilde{4}\sigma$	23.20	22.97	22.71	20.31	21.58	21.38	21.15
$\tilde{5}\sigma$	19.03	18.89	18.70	16.31	16.46	16.41	16.33
$\tilde{1}\pi$	18.13	18.02	17.87	15.48	16.32	16.20	16.05

[a]Ni$-N_a$ distance in bohr.

N_2 and Table V for NiN_2 [GS only; we have not yet succeeded in computing all I(relaxed) values for valence levels of GS(π)]. Tables IV and V also include the N 1s core-level IP's, although discussion of these is reserved for elsewhere.[9,12]

The I(relaxed) values for N_2 agree fairly well with the experimental IP's except for the reversal of the order of 5σ and 1π. This problem, found also in SCF calculations with very extended basis sets,[28] is due to a large differential correlation error between the $5\sigma^{-1}$ and $1\pi^{-1}$ ions. The $5\sigma^{-1}$ ion has substantially more correlation energy (neglected in the HF approximation) than does the $1\pi^{-1}$ ion. This can be seen from the fact that $I_{5\sigma}$(relaxed) is larger than $I_{5\sigma}$(expt.) rather than smaller, as is usually the case for the IP to the lowest ionic state.[29] It is important that we understand the origin of this large differential correlation if we are to make meaningful comparisons among the calculated IP's for N_2 and NiN_2 and the observed IP's for N_2 and Ni(100)/N_2.[9] It is reasonable to expect that internal[30] correlation effects involving the rather low-lying ("near-degenerate") $2\pi^*$ level of N_2 will account for a large part of the differential correlation between the $5\sigma^{-1}$ and $1\pi^{-1}$ states. We have tested this expectation with configuration-interaction (CI) calculations on the lowest $^2\Sigma_g^+ 5\sigma^{-1}$, $^2\Pi_u 1\pi^{-1}$, and $^2\Sigma_u^+ 4\sigma^{-1}$ states of N_2. The CI involved all symmetry-allowed states which could be formed by distributing the 9 N_2 valence electrons over the 3σ, 4σ, 5σ, 1π, and 2π MO's.[31] (The MO's were determined by HF calculations for the appropriate state of N_2 and the contracted Gaussian basis set described in Sec. II was used.) The CI results for the relative IP's of these three states are compared in Table VI with the experimental and SCF relative IP's. The inclusion of correlation effects involving only $2\pi^*$ not only corrects the ordering of the $5\sigma^{-1}$ and $1\pi^{-1}$ states, but also leads to reasonable agreement with experiment for the relative IP's. In Table VI we also give the $2\pi^*$ natural orbital (NO) occupation numbers[32,33] obtained from the CI wave functions for the three states. These occupation numbers clearly show the greater importance of the $2\pi^*$ level for the $5\sigma^{-1}$ and $4\sigma^{-1}$ states than for the $1\pi^{-1}$ state.

The consequences of this dramatic $2\pi^*$ correlation that are of interest here are as follows. Since in the NiN_2 cluster the N_2-like MO's retain much of their free molecule character, essentially the same correlation errors will occur for NiN_2 as for N_2. Therefore, in considering the theoretical IP *shifts* in going from N_2 to the NiN_2 cluster, the differential correlation effect will be very small and may be neglected. When we come to compare the NiN_2-N_2 *theoretical* results with the *experimental* Ni(100)/N_2-N_2 data, one may not be able to ignore differential correlation effects. In fact, this turns out to be an important consideration because the important correlating orbital is the $2\pi^*$ orbital which, as we have already suggested, is involved in the bonding to a real Ni surface. Therefore, the correlation effects in free N_2 will not be the same as for Ni(100)/N_2.[9]

Let us now consider the behavior of the calculated IP's for the NiN_2 cluster as a function of bond distance, and then the effect of the nickel-nitrogen interaction on the N_2-like IP's. The variation of I(Koopmans's) for the cluster ground state is quite small for the $\pm 5\%$ variation about the sum of the covalent radii (3.80 bohr) for all the IP's (Table V). The variation is significantly larger, however, for the $\tilde{4}\sigma$ and $\tilde{5}\sigma$ orbitals (0.49 and 0.33 eV, respectively) than for the other orbitals ($\sim$0.2 eV). This is because the $\tilde{4}\sigma$ and $\tilde{5}\sigma$ levels are involved in the NiN_2 bond and should therefore be more strongly affected by bond distance variations. The variation of I(relaxed) behaves in a similar fashion to I(Koopmans's), except that the value for $\tilde{5}\sigma$ is only 0.13 eV instead of the 0.33 eV of I(Koopmans's).

TABLE VI. Comparison among experimental, Hartree-Fock, and CI (see text) values for the 5σ, 1π, and 4σ relative IP's, in eV, for the free N_2 molecule. The $2\pi^*$ ($1\pi_g$) natural orbital occupation numbers are given for the CI wave functions.

Orbital	I(expt.)[a]	I(HF)	I(CI)	$2\pi^*$ NO Occupation
5σ	0	0	0	0.17
1π	1.3	−0.57	1.42	0.10
4σ	3.1	4.29	3.31	0.25

[a]K. Siegbahn *et al., ESCA Applied to Free Molecules* (North-Holland, Amsterdam, 1971).

This behavior is the first indication that there is something unusual about the $\tilde{5}\sigma^{-1}$ final state. Further evidence that $\tilde{5}\sigma^{-1}$ has some peculiarities which were not anticipated are presented later.

In order to study the effect of the nickel-nitrogen interaction on the N_2-like ionization potentials, it has proven useful[1] to define the following shifts, ΔE:

$$\Delta E_{\text{tot}} = I(\text{relaxed},N_2) - I(\text{relaxed},NiN_2)\ , \tag{4}$$

$$\Delta E_I = I(\text{Koopmans's},N_2) - I(\text{Koopmans's},NiN_2) \tag{5}$$

$$\Delta E_R = \Delta E_{\text{tot}} - \Delta E_I = E_R(NiN_2) - E_R(N_2)\ , \tag{6}$$

where E_R is the final-state relaxation energy for the molecule or the cluster. The initial-state shift ΔE_I consists of two contributions. First, a level may be shifted because it becomes involved in a bond to the Ni (bonding shift). Second, a level may be shifted by the changed environment in the cluster (environmental or chemical shift). The latter is the only initial-state shift to affect nonbonding levels. The relaxation shift ΔE_R arises because of the different final-state behavior of the free and the "adsorbed" N_2 molecule. In general, E_R will alway be greater in the "adsorbed" situation because of the additional availability of electrons to screen a final-state hole. The above decomposition of shifts is commonly (qualitatively) used for the analysis of experimental adsorbate shifts.[5,25,26] The present model calculation can give estimates of the magnitudes and behavior of the individual terms for different "adsorbate" levels of the cluster.

We must keep in mind here, though, that we are considering the linear cluster and not the real Ni surface-adsorbate situation, and also that in terms of physical observables there is no way to separate the ΔE_I and ΔE_R terms. One can only observe ΔE_{tot}. The shift contributions of our cluster model (computed from the IP's in Tables IV and V) are given in Table VII and compared to the equivalent results for NiCO.[1,7] The results for ΔE_I—discussed first—are qualitatively the same for all $d_{\text{Ni}-\text{N}_a}$ values. The ΔE_I at a given $d_{\text{Ni}-\text{N}}$ have negative values of roughly the same magnitude (~ 1.5 eV at $d_{\text{Ni}-\text{N}} = 3.65$ bohrs, ~ -1.4 eV at $d_{\text{Ni}-\text{N}} = 3.80$ bohrs, ~ -1.3 eV at $d_{\text{Ni}-\text{N}} = 4.0$ bohrs) for all but the $\tilde{4}\sigma$ and $\tilde{5}\sigma$ orbital. We have identified these two orbitals as bonding towards the nickel and therefore it is expected that their bonding shift should be larger than for the other orbitals. The value of $\Delta E_I(\tilde{5}\sigma)$ in NiN_2 is about half of that in NiCO while the value of $\Delta E_I(\tilde{4}\sigma)$ is 50% greater in NiN_2 than in NiCO. This is a consequence of the fact that both the $\tilde{4}\sigma$ and $\tilde{5}\sigma$ MO's are involved in the σ bonding to Ni in NiN_2, while only $\tilde{5}\sigma$ is involved in NiCO. Since the total σ bonding in NiN_2 is only slightly less than in NiCO, the bonding contribution to $\Delta E_I(\tilde{5}\sigma)$ must be smaller than in NiCO and that for $\Delta E_I(\tilde{4}\sigma)$ larger. Since $\tilde{3}\sigma$ is a "corelike" nonbonding MO, $\Delta E_I(\tilde{3}\sigma)$ is ascribed entirely to a chemical-shift effect. For the valence $\tilde{1}\pi$ MO, there is no rigorous way to make a quantitative separation between the bonding and the chemical contribution to ΔE_I. However, the charge distribution of $\tilde{1}\pi$ (from population analyses or orbital plots), together with the fact that $\Delta E_I(\tilde{1}\pi)$ is quite close to the value for the core orbitals, strongly suggests that the dominant contribution to ΔE_I is a chemical shift. The values of $\Delta E_I(\tilde{3}\sigma)$ and $\Delta E_I(\tilde{1}\pi)$ are larger in NiN_2

TABLE VII. Calculated level shifts, in eV, of the N_2 orbitals due to the interaction with nickel for three different nickel-nitrogen distances. The definitions of the initial- and final-state contributions ΔE_I and ΔE_R to the total shift ΔE_{tot} are given in the text.

	ΔE_{tot}				ΔE_I				ΔE_R			
Orbital	NiN_2			NiCO	NiN_2			NiCO	NiN_2			NiCO
	r[a]=3.65	3.80	4.00	3.477	3.65	3.80	4.00	3.477	3.65	3.80	4.00	3.477
$\tilde{1}\sigma(N_a\ 1s)$[b,c]	−0.64	−0.58	−0.48	−0.04	−1.51	−1.44	−1.32	−1.11	0.87	0.86	0.84	1.07
$\tilde{2}\sigma(N_b\ 1s)$[b,c]	−0.30	−0.33	−0.36	−0.13	−1.51	−1.44	−1.31	−1.39	1.21	1.11	0.95	1.26
$\tilde{3}\sigma$	−0.64	−0.60	−0.54	−0.19	−1.37	−1.30	−1.19	−1.01	0.73	0.70	0.65	0.82
$\tilde{4}\sigma$	−1.40	−1.21	−0.97	−1.12	−2.11	−1.88	−1.62	−1.17	0.71	0.67	0.65	0.05
$\tilde{5}\sigma$	−0.57	−0.53	−0.45	−2.88	−1.88	−1.75	−1.55	−3.27	1.31	1.22	1.10	0.39
$\tilde{1}\pi$	−0.99	−0.88	−0.73	−1.05	−1.50	−1.39	−1.24	−1.14	0.51	0.51	0.51	0.09

[a]Ni−N_a distance in bohrs.

[b]For NiCO, $\tilde{1}\sigma$ is the O 1s ion and $\tilde{2}\sigma$ is the C 1s ion.

[c]N_a denotes the N atom closest to Ni and N_b the N furthest away.

than in NiCO by $\sim 0.2-0.4$ eV, depending on distances. This increase is probably due to the fact that the charge in $\tilde{3}\sigma$ and $\tilde{1}\pi$ is about equally distributed on N_a and N_b in NiN_2 whereas it is strongly localized on O in NiCO.

The ΔE_I data for all orbitals in Table VII go towards smaller absolute values with increasing d_{Ni-N} as expected. However, the variations are clearly larger for the bonding $\tilde{4}\sigma$ and $\tilde{5}\sigma$ orbitals compared to the others, which indicates that the bonding contribution to ΔE_I dies off much faster with increasing distance than the chemical-shift contribution. The behavior of ΔE_R is strikingly different for all of the valence levels, for NiN_2 compared to NiCO. To help us explain these differences, we have summarized in Table VIII some properties of the N_2-derived valence orbitals of NiN_2^+.

The value of $\Delta E_R \tilde{5}\sigma$ for NiN_2, 1.1 eV, is almost three times larger than that for NiCO. This large ΔE_R can be understood by comparing the $\tilde{4}\sigma$ and $\tilde{5}\sigma$ MO characteristics for the NiN_2-ionized $\tilde{5}\sigma^{-1}$ state (Table VIII) with those of the ground state (Tables IIB and III). The ionized-state orbitals are considerably different from those of the ground state. In the ion, all of the σ bonding to Ni is now concentrated in the doubly occupied $\tilde{4}\sigma$ MO and the singly occupied $\tilde{5}\sigma$ MO has become a nonbonding orbital whose charge is almost entirely on N_b. Thus, the relaxed $\tilde{5}\sigma^{-1}$ ion state is very different from the Koopmans's ion state where the hole is made in one of two σ-bonding MO's, and these MO's are not allowed to change their character. In effect this means that the photoemission process cannot be described in terms of a one-electron transition from the $\tilde{5}\sigma$ orbital. It is this huge change in the character of the $\tilde{5}\sigma$ orbital upon ionization, effectively localizing it on N_b, which leads to the large $\Delta E_R(\tilde{5}\sigma)$. By localizing on a lone-pair nonbonding-type orbital on N_b, the ionization process is made easier than it would otherwise be. Hence the IP is much lower than expected from the $-\epsilon_{\tilde{5}\sigma}$ value and thus ΔE_R is very large. In the ionized state the $\tilde{5}\sigma^{-1}$ orbital of NiN_2 has a spatial distribution which is rather similar to the $\tilde{4}\sigma^{-1}$ of NiCO (or indeed of CO itself).

We would expect a large rearrangement of the $\tilde{4}\sigma$ and $\tilde{5}\sigma$ orbitals for the $\tilde{4}\sigma^{-1}$ final state of NiN_2^+ also, since this state must be orthogonal to $\tilde{5}\sigma^{-1}$. The Ni $\tilde{4}\sigma^{-1}$ should become a localized $Ni-N_a$ bonding orbital which is singly occupied, while the $\tilde{5}\sigma$ orbital should be a doubly occupied lone pair on N_b. This would drive the $\tilde{4}\sigma$ IP up and so $\Delta E_R(\tilde{4}\sigma^{-1})$ would be expected to be very small or even negative. In fact, this does not happen in the calculations. In the $\tilde{4}\sigma^{-1}$ state, the $\tilde{5}\sigma$

TABLE VIII. Properties of the N_2-like valence MO's in the ionic wave functions. The ionic states are denoted as $n\lambda^{-1}$.

Ionic state	Orbital	$\langle z \rangle_{N_a}$	Gross population Ni	Gross population N_a	Gross population N_b	Overlap population $Ni-N_a$	Overlap population N_a-N_b
$\tilde{5}\sigma^{-1}$	$\tilde{3}\sigma$	1.041	−0.01	0.46	0.55	−0.01	0.39
	$\tilde{4}\sigma$	−0.382	0.03	0.87	0.10	0.04	−0.24
	$\tilde{5}\sigma$	2.266	0.03	0.07	0.90	0.00	−0.10
	$\tilde{1}\pi$	1.136	0.00	0.45	0.55	0.00	0.24
$\tilde{4}\sigma^{-1}$	$\tilde{3}\sigma$	1.034	−0.01	0.47	0.53	−0.01	0.40
	$\tilde{4}\sigma$	0.781	0.01	0.54	0.44	0.02	−0.27
	$\tilde{5}\sigma$	1.157	0.03	0.42	0.55	0.03	−0.01
	$\tilde{1}\pi$	0.950	0.00	0.53	0.46	0.00	0.24
$\tilde{1}\pi^{-1}$	$\tilde{3}\sigma$	1.026	−0.01	0.47	0.53	−0.01	0.39
	$\tilde{4}\sigma$	0.427	0.02	0.64	0.33	0.03	−0.36
	$\tilde{5}\sigma$	1.553	0.02	0.31	0.67	0.01	−0.03
	$\tilde{1}\pi$	0.802	0.03	0.54	0.43	0.01	0.24
$\tilde{3}\sigma^{-1}$	$\tilde{3}\sigma$	1.017	−0.01	0.46	0.54	−0.01	0.36
	$\tilde{4}\sigma$	0.308	0.03	0.67	0.31	0.03	−0.37
	$\tilde{5}\sigma$	1.678	0.01	0.29	0.69	0.01	−0.01
	$\tilde{1}\pi$	0.975	0.00	0.53	0.47	0.00	0.25

orbital actually has *less* N_b lone-pair character than it does in the ground state. This fault in the calculation happens because in a SCF calculation there is no constraint of orthogonality among different states of the same symmetry and so the $\widetilde{4}\sigma^{-1}$ state tries to mimic the ground ionized state, $\widetilde{5}\sigma^{-1}$. Thus the calculated $\Delta E_R(\widetilde{4}\sigma^{-1})$ of ~ 0.7 eV is too large because the orthogonality of $\widetilde{4}\sigma^{-1}$ to $\widetilde{5}\sigma^{-1}$ is not properly included.

When making our comparison to experiment, we will see (following paper) that the important factor in the theory is that the sum of the initial- and final-state shifts, ΔE_{tot}, are such that the I(Relaxed) values for the $\widetilde{4}\sigma$ and $\widetilde{5}\sigma$ levels of NiN_2 are pushed further apart than they are for N_2. The calculated increase is 0.7 eV. If the orthogonality problem were properly accounted for, ΔE_R $(\widetilde{4}\sigma^{-1})$ would be smaller and the $\widetilde{4}\sigma - \widetilde{5}\sigma$ IP separation would increase by *more* than 0.7 eV on going from N_2 to NiN_2. This is the reverse of the behavior for the NiCO cluster where the $\widetilde{5}\sigma$ and $\widetilde{4}\sigma$ IP's get *closer* together compared to CO (by 1.8 eV; see Table VI).

The reason for the different behavior in NiCO is simply that in the NiCO cluster the $\widetilde{5}\sigma$ and $\widetilde{4}\sigma$ orbitals are *already* localized into a bonding orbital between Ni and C (the $\widetilde{5}\sigma$), and a lone-pair nonbonding orbital on O ($\widetilde{4}\sigma$) in the ground state of the cluster (as indeed they are also for free CO because of the difference in nuclear charge on the C and O atoms). Thus, in the final ionized states no dramatic rearrangement occurs and the Koopmans's one-electron picture of ionization from $\widetilde{5}\sigma$ and $\widetilde{4}\sigma$ has considerable validity. Since $\widetilde{5}\sigma$ is strongly bonding in NiCO, it is much harder to remove an electron from it than from the $\widetilde{5}\sigma$ orbital of free CO. Therefore the $\widetilde{5}\sigma$ IP is pushed *up* closer to $\widetilde{4}\sigma$ in NiCO compared to that in free CO.

The values of ΔE_R $(\widetilde{3}\sigma^{-1})$ and ΔE_R $(\widetilde{1}\pi^{-1})$ are nearly constant at 0.7 and 0.5 eV, respectively, for all $Ni-N_a$ distances shown in Table VI. This constancy reflects the nonbonding character of these MO's. The value of ΔE_R $(\widetilde{3}\sigma^{-1})$ for NiN_2 is only slightly smaller than for NiCO. For $\widetilde{1}\pi$, however, ΔE_R is much larger in NiN_2 than in NiCO. This follows from the fact that $\widetilde{1}\pi$ in NiN_2 (see Tables IIB, III, and VIII) is distributed about equally on both N_a and N_b while in NiCO, $\widetilde{1}\pi$ is strongly localized on the O center.

Most of the preceding discussion in this section has concerned an explanation of the effects of the N_2-like IP's when the N_2 is bonded to Ni in the linear cluster in the *cluster ground state.* We showed, however, in Sec. III A that Ni $4p\pi$-$N_2 2\pi^*$ backbonding must be significant for a real Ni surface-N_2 interaction, and that to model this interaction in a linear cluster it is necessary to use the GS(π) of the cluster, not GS. Since we believe that the GS(π) cluster rather than the GS cluster is necessary to model the interaction on a real Ni surface, we would expect the experimental IP's for the NiN_2 system to agree more closely with those obtained from IP calculations on the GS(π) of the NiN_2 cluster. Thus, we must consider the differences in the behavior of the calculated IP's for ionization from the GS(π) cluster compared to those from the GS cluster.

We can estimate what these values for valence-level ionization might be, based on the calculations for the GS(π) initial state and for the I(Relaxed) for GS. As mentioned in Sec. III A, the major effect of allowing the $4p\pi$-$2\pi^*$ interaction by using GS(π) is to increase all the valence-level N_2-derived orbital eigenvalues by approximately 2.4 eV and decrease the Ni-derived orbital eigenvalues by approximately 0.8 eV compared to the GS values for ϵ. As shown in Table V, the GS(π) values of I(Koopmans's) for the valence levels are decreased by a slightly larger amount, 2.5–2.7 eV. [This is because, as discussed above, the multiplet splittings are larger for GS(π) than for GS.] The physical reason for this rigid shift to lower IP is straightforward; it arises because the $4p\pi \rightarrow 2\pi^*$ backbonding interaction transfers charge to the N_2 end of the cluster. The most simple estimate that we can make for the I(relaxed) for GS(π) is that they are the GS values for I(relaxed) decreased by the same amount that the I(Koopmans's) are decreased[34]:

$$I(\text{relaxed;GS}(\pi)) \cong I(\text{relaxed;GS}) - 2.5 \text{ eV} .$$

IV. CONCLUSIONS

The HF calculations on the GS of the linear NiN_2 cluster have revealed a significant but not unexpected difference in the bonding mechanism compared to that in the previously studied NiCO cluster. Whereas the bonding in the latter is almost entirely through the $\widetilde{5}\sigma$ lone pair on the carbon atom, in the former it is almost equally split between the $\widetilde{5}\sigma$ and $\widetilde{4}\sigma$ orbitals which are both delocalized over the whole N_2 molecule. In addition, the bonding is weaker in the NiN_2 cluster. In

terms of experimental observables, the difference between the two systems translates into an *increase* in separation between $\tilde{5}\sigma$ and $\tilde{4}\sigma$ IP's for N_2 going to NiN_2 and a *decrease* for CO going to NiCO. The difference comes about essentially because in the latter case both initial and final states in the photoemission process have 5σ and 4σ localized lone-pair-like orbitals. There are therefore no large differential final-state relaxation effects and the $\tilde{5}\sigma^{-1}$ IP moves to a higher value because of the initial-state bonding of 5σ to the Ni atom. In the case of NiN_2, the delocalized $\tilde{5}\sigma$ and $\tilde{4}\sigma$ orbitals both become strongly localized in each of the $\tilde{5}\sigma^{-1}$ and $\tilde{4}\sigma^{-1}$ final states. Differential relaxation effects then make the $\tilde{5}\sigma^{-1}$ IP lower than would otherwise be expected and the $\tilde{4}\sigma^{-1}$ higher, thus pushing the IP's further apart.

We also performed HF calculations on the GS(π) of NiN_2 because we wish in the following paper[9] to make comparisons to the Ni(100)/N_2 adsorption system and we know from the core-level XPS of the system that Ni $4p\pi \rightarrow 2\pi^*$ backbonding plays a significant role. This interaction is symmetry-excluded in the GS of the linear NiN_2 cluster, but is allowed in the GS(π). The latter therefore serves as a model for qualitatively establishing what effects the $4p\pi \rightarrow 2\pi^*$ interaction will have on bonding in the system and on the observables (the IP's). We find that there is a significant $4p\pi$-$2\pi^*$ contribution to the total bond strength and that the GS(π) cluster is stable with respect to its dissociation products by some 1.13 eV, whereas the GS cluster is only about 0.1 eV stable. [It has been found on a Cu_5CO cluster that a state which is similar to the GS(π) is, in fact, the true cluster ground state, which further justifies our use of the GS(π) NiN_2 here to model the Ni/N_2 interaction.[24]] The N_2-derived valence ionization potentials of the GS(π) cluster are estimated, on the basis of initial-state effects, to be about 2.5 eV lower than those of the GS because of the charge transfer from Ni to N_2 caused by the $4p\pi \rightarrow 2\pi^*$ interaction.

The final major point concerns the effect of electron correlation. The neglect of correlation in the HF calculation causes a reversal of the experimental order of IP's of N_2 ($5\sigma, 1\pi, 4\sigma$) compared to the HF result ($1\pi, 5\sigma, 4\sigma$) because the degree of correlation is much greater for the $5\sigma^{-1}$ final state than the $1\pi^{-1}$ final state. This, we have shown, comes about essentially because of configuration mixing with the low-lying empty $2\pi^*$ orbital. The correct ordering can be retrieved by a simple internal CI calculation. In the case of NiN_2, GS, a very similar HF correlation error is to be expected since the N_2-derived orbitals retain so much of their free-molecule character. However, in any comparison to the Ni(100)/N_2 experimental IP's, it might be expected that the correlation error of the NiN_2 calculation would be of less significance than for the comparison of experimental N_2 IP's to HF IP's since for Ni(100)/N_2 we have shown that the $2\pi^*$ orbital is partially occupied and therefore not available for correlation. Thus we would anticipate that the *relative* IP's of $\tilde{5}\sigma^{-1}$ and $\tilde{1}\pi^{-1}$ for Ni(100)/N_2 would be more accurately reproduced by an HF calculation (which neglects correlation) for NiN_2 than are the relative IP's of N_2 reproduced by an HF calculation on N_2.

ACKNOWLEDGMENT

Two of us (K.H. and D.M.) would like to express our gratitude to IBM, Germany for having provided support which made possible our stay at the IBM Research Laboratory, San Jose.

*Permanent address: Inst. für Theor. Physik B, TU Clausthal, 3392 Clausthal West Germany and Sonderforschungsbereich 126, Clausthal/Göttingen.

†Permanent address: Inst. für Festkörperphysik, TU München, 8046 Garching, West Germany.

[1]K. Hermann and P. S. Bagus, Phys. Rev. B 16, 4195 (1977).

[2]For a brief discussion and reference to the various interpretations of CO/Ni, see Ref. 1.

[3]I. P. Batra and P. S. Bagus, Solid State Commun. 16, 1097 (1975).

[4]D. R. Lloyd, Discuss. Faraday Soc. 58, 136 (1974).

[5]J. E. Demuth and D. E. Eastman, Phys. Rev. Lett. 32, 1123 (1974).

[6]T. Gustafsson, E. W. Plummer, D. E. Eastman, and J. L. Freeouf, Solid State Commun. 17, 391 (1975); J. C. Fuggle, T. E. Madey, M. Steinkilberg, and D. Menzel, Phys. Lett. 51A, 163 (1975); J. C. Fuggle, M. Steinkilberg, and D. Menzel, Chem. Phys. 11, 307 (1975).

[7]P. S. Bagus and K. Hermann, Solid State Commun. 20, 5 (1976).

[8](a) J. C. Fuggle and D. Menzel, in *Proceedings of the Seventh International Vacuum Congress and the Third International Conference on Solid Surfaces* (IVC, Vienna, 1977); (b) J. C. Fuggle, E. Umbach, D. Menzel, K. Wandelt, and C. R. Brundle, Solid State Commun. 27, 65 (1978); (c) E. Umbach, A. Schichl, and D. Menzel, Solid State Commun. 36, 93 (1980).

[9]C. R. Brundle, P. S. Bagus, D. Menzel, and K. Hermann, J. Electron Spectrosc. Relat. Phenom. 20, 253 (1980), and Phys. Rev. B 24, 7041 (1981), following paper.

[10](a) K. Schönhammer and O. Gunnarsson, Solid State Commun. 23, 691 (1977); (b) 26, 399 (1978).

[11]P. S. Bagus and K. Hermann, Surf. Sci. 89, 588 (1979).

[12]K. Hermann and P. S. Bagus, Solid State Commun. 38, 1257 (1981).

[13]J. C. Slater, *Symmetry and Energy Bands in Crystals* (Dover, New York, 1972).

[14]*Handbook of Chemistry and Physics,* 56th ed., edited by R. C. Weast (CRC, Cleveland, 1975).

[15]The MOLALCH program package incorporates the MOLECULE integral program and the ALCHEMY SCF program. MOLECULE was written by J. Almlöf of the University of Uppsala, Sweden. The ALCHEMY SCF program was written by P. S. Bagus and B. Liu of the IBM Research Laboratory, San Jose. The interfacing of these programs was performed by U. Walgren, University of Uppsala, and P. S. Bagus at IBM. The wave-function contour plot part was written by K. Hermann.

[16]F. B. van Duijneveldt, IBM Research Report No. RJ945, unpublished.

[17]Following B. Roos and P. Siegbahn, Theor. Chim. Acta 17, 199 (1970).

[18]A. J. H. Wachters, J. Chem. Phys. 52, 1033 (1970).

[19]H. F. Schaefer, III, *The Electronic Structure of Atoms and Molecules* (Addison-Wesley, Reading, Massachusetts, 1972).

[20]R. S. Mulliken, J. Chem. Phys. 23, 1833 (1955); 23, 1841 (1955); 23, 2338 (1955); 23, 2343 (1955).

[21]H. H. Maden, J. Küppers, and G. Ertl, J. Chem. Phys. 57, 3041 (1973).

[22]D. A. King, Surf. Sci. 9, 375 (1968).

[23]In our calculations we do not require full spatial symmetry ($C_{\infty v}$) and equivalence restrictions. Thus the state of Eq. (3) is pure spin triplet, but its spatial symmetry is a combination of Δ and Φ symmetry.

[24]It has been shown for Cu [P. S. Bagus and M. Seel, Phys. Rev. B 23, 2065 (1981)] that if one takes a cluster of five Cu atoms, the *ground* state of this cluster does indeed contain significant $p\pi$ character and that this character does couple to the $2\pi^*$ level of CO when a Cu_5CO cluster is formed. This further justifies the use of the excited Ni-atom configuration $3d^9 4p\pi$ in the linear cluster calculation when comparing to experiment on Ni(100). Walch and Goddard [J. Am. Chem. Soc. 98, 7908 (1976)] have shown that correlation effects, neglected in HF calculations, lead to a significant improvement in the total energy of the ground state of a NiCO cluster and we may expect similar effects for NiN_2. If we were primarily interested in the best total energy for the linear cluster ground state, then we should undoubtedly consider these correlation corrections. However, since all of the discussion so far indicates that the $4sp-2\pi^*$ coupling is the dominant difference of the real Ni surface from the ground-state linear cluster, we consider it of greater importance to include this interaction in an HF calculation [i.e., GS(π)] than to make correlation corrections to GS.

[25]C. R. Brundle, *Proceedings of the NATO Advanced Study Institute on Electronic Structure and Reactivity of Metal Surfaces, Namur,* edited by E. G. Derouane and A. A. Lucas (Plenum, New York, 1976), p. 389.

[26]D. Menzel, in *Photoemission and the Electronic Properties of Surfaces,* edited by B. Feuerbacher, E. Fitton, and R. F. Willis (Wiley, London, 1978), p. 393.

[27]P. A. Cox, Mol. Phys. 30, 389 (1972).

[28]See, e.g., P. E. Cade, K. D. Sales, and A. C. Wahl, J. Chem. Phys. 44, 1973 (1966).

[29]R. S. Mulliken, J. Chim. Phys. 46, 497 (1949).

[30]H. J. Silverstone and O. Sinanoglu, J. Chem. Phys. 44, 1899 (1966) and references therein.

[31]For a more detailed description of this CI procedure, see P. S. Bagus and E. -K. Viinikka, Phys. Rev. A 15, 1486 (1977).

[32]P. O. Löwdin, Phys. Rev. 97, 1474 (1955).

[33]E. R. Davidson, Rev. Mod. Phys. 44, 451 (1972).

[34]Since completing this paper some results have been obtained for I(Relaxed;GS(π)) for the valence levels. They are included in the comparison to experiment in the following paper. They do not follow the simple prediction given here, essentially because both screened and unscreened valence-level final states are found to have significant intensities whereas I(Relaxed;GS) has intensity only into the unscreened final states; see P. S. Bagus, K. Hermann, and M. Seel, J. Vac. Sci. Technol. 18, 435 (1981).

[35]R. K. Nesbet, Proc. R. Soc. London Ser. A 230, 312 (1955).